Experimental proof-of-principle investigation of enhanced $Z_{3D}T$ in (001) oriented Si/Ge superlattices

T. Koga[a)]
Division of Engineering and Applied Sciences, Harvard University, Cambridge, Massachusetts 02138

S. B. Cronin and M. S. Dresselhaus[b)]
Department of Physics, Massachusetts Institute of Technology, Cambridge, Massachusetts 02139

J. L. Liu and K. L. Wang
Electrical Engineering Department, UCLA, Los Angeles, CA 90095-1597

(Received 16 June 2000; accepted for publication 7 July 2000)

An experimental proof-of-principle of an enhanced $Z_{3D}T$ (thermoelectric figure of merit) is demonstrated using (001) oriented Si/Ge superlattices. The highest value of the experimental $Z_{3D}T$ at 300 K for a (001) oriented Si(20 Å)/Ge(20 Å) superlattice is 0.1 using $\kappa = 5\ \mathrm{Wm^{-1}K^{-1}}$, for the in-plane thermal conductivity, which is a factor of seven enhancement relative to the estimated value of $Z_{3D}T = 0.014$ for bulk Si. The good agreement between experiment and theory validates our modeling approach (denoted as ''carrier pocket engineering'') to design superlattices with enhanced values of $Z_{3D}T$. Proposals are made to enhance the experimental values of $Z_{3D}T$ for Si/Ge superlattices even further. © *2000 American Institute of Physics.* [S0003-6951(00)05136-6]

The use of low-dimensional structures, as realized in the form of two-dimensional (2D) quantum wells[1–15] and one-dimensional (1D) quantum wires,[16–20] has been shown to provide a promising strategy for designing materials with a large value of the thermoelectric figure of merit ZT. The original predictions of enhanced ZT for isolated quantum wells and/or wires (denoted by $Z_{2D}T$ and $Z_{1D}T$, respectively) used a simple model based on the constant relaxation time approximation (CRTA).[1,16] Although the predictions of enhanced $Z_{2D}T$s within the quantum wells were experimentally verified using the (111) oriented PbTe/$Pb_{1-x}Eu_x$Te multiple quantum well[3–5] and Si/SiGe superlattice (SL) systems[20,21] utilizing very thick barriers to isolate the neighboring quantum wells electrically, the main efforts in this research area are now shifted toward enhancing the value of $Z_{3D}T$, which denotes the thermoelectric figure of merit for the whole [three-dimensional (3D)] superlattice.

Recently, a general optimization approach to maximize the value of $Z_{3D}T$ using the superlattice structures, as denoted by the term ''carrier pocket engineering,'' was proposed, whereby the structures and geometries of a given superlattice system are optimized in such a way that the optimized structure maximizes the values of $Z_{3D}T$. The use of unconventional X and L valleys was proposed for the GaAs/AlAs superlattice system, and $Z_{3D}T = 0.4$ was predicted for both (001) and (111) oriented GaAs(20 Å)/AlAs(20 Å) SLs at 300 K.[12] For Si/Ge SLs, yet another new concept, that of lattice strain engineering, was proposed using strain-nonsymmetrized SLs, where $Z_{3D}T = 0.78$ and 1.25 are predicted for a (001) oriented Si(20 Å)/Ge(20 Å) SL and for a (111) oriented Si(15 Å)/Ge(40 Å) SL, respectively, at 300 K.[13,14] However, with the current molecular beam epitaxy (MBE) technology, it is not possible to grow strain-nonsymmetrized SLs with satisfactory structural qualities for thermoelectric applications. The values of $Z_{3D}T$ for strain-symmetrized (001) and (111) oriented Si(20 Å)/Ge(20 Å) SLs are predicted to be 0.24 and 0.96 at 300 K, respectively, using a simple model based on the constant relaxation time approximation (CRTA).[13,14]

In this letter, the experimental proof-of-principle study of the enhanced values of $Z_{3D}T$ is presented using MBE-grown strain-symmetrized Si(20 Å)/Ge(20 Å) SLs. The growth direction for all the superlattice samples used in the present study is the (001) direction, since the optimization of the growth conditions for the (111) oriented strain-symmetrized Si/Ge SLs has not been carried out yet.

The growth of the (001) oriented Si(20 Å)/Ge(20 Å) superlattices used in the present study are briefly described as follows. Typically, 100 periods of alternating layers of Si(20 Å) and Ge(20 Å) were grown on top of a 0.3–0.5-μm-thick $Si_{0.5}Ge_{0.5}$ undoped buffer layer. This undoped buffer layer was, in turn, grown on a 1–2-μm-thick $Si_{1-x}Ge_x$ (x:0→0.5) graded buffer layer using antimony as a surfactant[22] (surfactant-mediated growth). The $Si_{1-x}Ge_x$ graded buffer layers were grown both on a slightly p-type doped (001) Si substrate (samples JL167 and JL169) and on a (001) oriented Si-on-insulator (SOI) substrate (samples JL193, JL194, JL197, and JL199). The reason why we use SOI substrates in addition to (001) Si substrates is to avoid a large contribution of the phonon drag effect from the Si substrate to the measured Seebeck coefficient S below 200 K that masks the contribution to S from the superlattice part of the sample.[20,23,24]

Shown in Fig. 1(a) are the experimentally measured Seebeck coefficient (as-measured values are plotted using open circles) as a function of the Hall carrier concentration (n_{Hall}) at 300 K for the (001) oriented Si(20 Å)/Ge(20 Å) superlattice samples. In the present work, we assume that n_{Hall} is

[a)]Present address: NTT Basic Research Laboratories, Morinosato-Wakamiya, Atsugi-city, Kanagawa, 243-0198, Japan.
[b)]Also with: Department of Electrical Engineering and Computer Science; electronic mail: millie@mgm.mit.edu

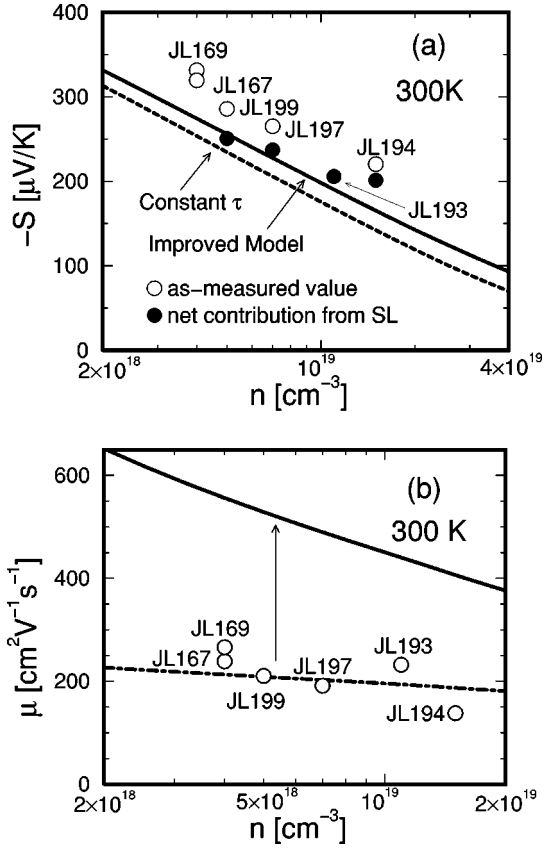

FIG. 1. (a) The Seebeck coefficient S and (b) the Hall carrier mobility μ as a function of the carrier concentration at 300 K for the (001) oriented strain-symmetrized Si(20 Å)/Ge(20 Å) superlattices. In (a) and (b), the open circles denote the as-measured (experimental) values for S and μ, respectively. The closed circles, in (a), denote the experimental values of S for the superlattice part of the sample only, after subtracting the buffer layer contribution to the measured S according to Eq. (2). In (a), the dashed and solid curves, respectively, denote the theoretically predicted values for S using the constant relaxation time approximation and those using the improved theoretical model, including $\tau_{ext}=4.0\times10^{-14}$ s in Eq. (1) [see (b)]. In (b), the dash-dotted curve and the solid curve, respectively, denote the theoretical results for μ using the improved model with and without including the τ_{ext} term in Eq. (1), where $\tau_{ext}=4.0\times10^{-14}$ s is obtained by fitting the experimental μ_{Hall} data (dash-dotted curve).

equal to the actual carrier concentration n, since the constant energy surface for these superlattice samples is circular (isotropic) and the geometric factor to convert n_{Hall} to n is equal to unity in this case.[23,25] It is found, in Fig. 1(a), that the measured values for the Seebeck coefficient are significantly larger than the values predicted by a model based on the CRTA [see the dashed curve in Fig. 1(a)]. The possible causes for this discrepancy between theory and experiment are explained as follows: (1) ionized impurity scattering, which is the dominant scattering mechanism for the superlattice samples used in the present study, gives rise to an increase in the value of $|S|$, relative to that predicted by the CRTA, through its preferable dependence of the relaxation time function, $\tau(E)$, on energy, and (2) the as-measured values of $|S|$ for the superlattice samples used in the present study tend to be larger than the net values of $|S|$ that are attributed to the superlattice part of the sample only, due to the parallel transport contribution from the $Si_{1-x}Ge_x$ buffer layers and/or Si substrate. To resolve the factor (1), we have developed an improved theoretical model for S based on the Boltzmann transport theory, including ionized impurity scattering and longitudinal acoustic phonon deformation potential scattering, where the effect of free-carrier screening is also included.[23] We use the Matthiessen's rule

$$\frac{1}{\tau_{tot}(E)}=\frac{1}{\tau_{imp}(E)}+\frac{1}{\tau_{ac}(E)}+\frac{1}{\tau_{ext}} \tag{1}$$

to include the scattering mechanisms that are extrinsic to the properties of the ideal strain-symmetrized Si/Ge superlattices. These scattering mechanisms (denoted by τ_{ext}) include scattering due to the interface roughness and that due to the structural defects and dislocations. It is also noted that the values for $\tau_{imp}(E)$ (associated with ionized impurity scattering) and $\tau_{ac}(E)$ (associated with longitudinal acoustic phonon deformation potential scattering) are calculated without the use of any fitting parameters by solving the Boltzmann equation using the literature values for the band parameters of bulk Si and Ge,[23] whereas the value for τ_{ext} is obtained by fitting the experimental results for the carrier mobility for the superlattice samples as a function of carrier concentration at 300 K as shown in Fig. 1(b). The predicted values for $|S|$ thus obtained are plotted by the solid curve in Fig. 1(a). To resolve the second reason for the discrepancy between theory (CRTA) and experiment (as-measured S) [see (2) above], we have employed a simple parallel-conductor model to subtract the buffer layer contribution to the measured $|S|$ [denoted by $S^{(buf.)}$] from the as-measured values for $|S|$ [denoted by $S^{(a.s.)}$] to evaluate the net contribution to the measured $|S|$ from the superlattice part of the sample only [denoted by $S^{(SL)}$]

$$S^{(SL)}=\frac{S^{(a.s)}\sigma_{\square}^{(a.s)}-S^{(buf.)}\sigma_{\square}^{(buf.)}}{\sigma_{\square}^{(a.s)}-\sigma_{\square}^{(buf.)}}, \tag{2}$$

where $\sigma_{\square}^{(a.s)}$ and $\sigma_{\square}^{(buf.)}$ are, respectively, the electrical sheet conductivity (electrical conductance per unit area) for the superlattice samples, including the buffer layer contribution and that for the bare buffer layer sample (a sample with only the buffer layers that are identical with those used for the growth of the samples JL193, JL194, JL197, and JL199). The net values of the Seebeck coefficient for the superlattice part of the sample thus obtained are plotted using the filled circles in Fig. 1(a). It is noted that the subtraction of the buffer layer contribution to estimate the values of $S^{(SL)}$ was not able to be carried out for samples JL167 and JL169, since the transport properties of the bare buffer samples for these superlattices [the $Si_{1-x}Ge_x$ buffer layers grown on (001) Si substrates directly] were not measurable due to their large impedances.

Shown in Fig. 2 is the experimentally determined thermoelectric power factor $S^2\sigma$ after subtracting the buffer layer contributions as discussed earlier (filled circles), together with the results of the theoretical predictions, as a function of carrier concentration n at 300 K. It is noted that the theoretical values for $S^2\sigma$ using the improved theoretical models discussed earlier without including the $1/\tau_{ext}$ term are plotted using the solid curve, whereas those obtained including the $1/\tau_{ext}$ term in the Matthiessen's rule are plotted using the dash-dotted curve. The former (solid curve) of the theoretical results for $S^2\sigma$ is considered to represent the intrinsic properties of the homogeneously doped (001) oriented Si(20 Å)/Ge(20 Å) SLs, where the extrinsic mechanisms for scat-

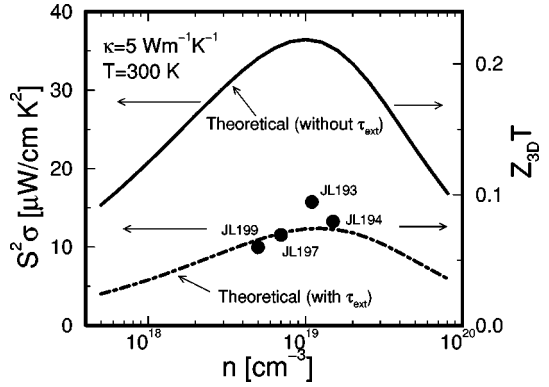

FIG. 2. The experimentally determined as well as theoretically predicted thermoelectric power factor $S^2\sigma$ (left scale) as a function of carrier concentration at 300 K for the (001) oriented Si(20 Å)/Ge(20 Å) superlattice samples. The experimental results for $S^2\sigma$ vs n shown here are those after the subtraction of the buffer layer contribution according to Eq. (2) (filled circles). The theoretical curves shown here are obtained using the improved theoretical model with (dash-dotted curve) and without (solid curve) including the τ_{ext} term in Eq. (1), where $\tau_{ext}=4.0\times10^{-14}$ s is obtained in Fig. 1(b). The right scale in the figure shows the corresponding values for $Z_{3D}T$ using $\kappa=5$ W/m K for the thermal conductivity.

tering carriers, such as the scattering due to the interface roughness and/or due to the structural defects or dislocations, are absent. Therefore, the experimental values for $S^2\sigma$ for the (001) oriented Si/Ge superlattice samples obtained in this study ($S^2\sigma<16\mu\,\mathrm{W\,cm^{-1}K^{-2}}$) can be expected to increase further (by a factor of up to 2–3) by improving the structural quality of the superlattices ($S^2\sigma\approx36\ \mu\mathrm{W\,cm^{-1}\,K^{-2}}$). It is also noted that the values of $S^2\sigma$ are predicted to increase even further ($S^2\sigma>36\ \mu\mathrm{W\,cm^{-1}\,K^{-2}}$) by introducing the δ- and modulation-doping schemes in (001) oriented Si(20 Å)/Ge(20 Å) SLs.[23]

To make an order of magnitude estimation for the value of the experimental $Z_{3D}T$, we attach an additional scale for $Z_{3D}T$ on the right hand side of Fig. 2, using a constant value of $\kappa_{\|}=5$ W/m K for the in-plane (parallel to the planes of the superlattices) thermal conductivity for the pertinent SLs. This value for $\kappa_{\|}$ (5 W/m K) is chosen considering the fact that the experimentally determined values for the crossplane (along the direction perpendicular to the superlattice planes) thermal conductivity (denoted by $\kappa_{\perp}$) are in the range between 1 and 2 W/m K for samples JL194, JL197, and JL199,[26] whereas the most conservative estimation for the value of $\kappa_{\|}$ using the Si/Ge superlattice sample that has the smallest dislocation density (sample JL156) turns out to be $\kappa_{\|}=12$ W/m K at 300 K using the models proposed by Chen.[27–29] In Fig. 2, we indeed see a several fold enhancement in the measured values of $Z_{3D}T(\approx0.08)$ in these (001) oriented Si(20 Å)/Ge(20 Å) SL samples relative to the corresponding value for $Z_{3D}T$ for bulk Si ($Z_{3D}T\approx0.014$), and the values of $Z_{3D}T$ for these SLs are expected to be increased further by improving the structural quality of the superlattices as discussed above.

In summary, an experimental proof-of-principle study of an enhanced thermoelectric figure of merit $Z_{3D}T$ has been carried out using (001) oriented Si/Ge superlattices to test the reliability of our modeling approach denoted by the carrier pocket engineering concept. We find that the experimental values of $Z_{3D}T$ for (001) oriented Si(20 Å)/Ge(20 Å) superlattices are as high as 0.1 at 300 K, which is about a sevenfold enhancement relative to the corresponding value for bulk Si ($Z_{3D}T=0.014$). The successful experimental proof-of-principle study of enhanced $Z_{3D}T$ using the (001) oriented Si(20 Å)/Ge(20 Å) superlattices suggests that practically useful values of $Z_{3D}T$ ($Z_{3D}T>1$) that are predicted for (111) oriented Si/Ge SLs[13] are also realizable in experiments. In addition, it is expected that the introduction of the δ- and modulation-doping schemes would increase the values of $Z_{3D}T$ for (111) oriented Si/Ge SLs even further, looking to a value of $Z_{3D}T\approx2$ at 300 K.

The authors would like to thank Professor G. Chen, T. Borca-Tasciuc, and Dr. G. Dresselhaus for valuable discussions. The authors gratefully acknowledge support from ONR under MURI Subcontract No. 205-G-7A114-01 and the U.S. Navy under Contract No. N00167-98-K-0024.

[1] L. D. Hicks and M. S. Dresselhaus, Phys. Rev. B **47**, 12727 (1993).
[2] L. D. Hicks, T. C. Harman, and M. S. Dresselhaus, Appl. Phys. Lett. **63**, 3230 (1993).
[3] T. C. Harman, D. L. Spears, and M. J. Manfra, J. Electron. Mater. **25**, 1121 (1996).
[4] L. D. Hicks, T. C. Harman, X. Sun, and M. S. Dresselhaus, Phys. Rev. B **53**, R10493 (1996).
[5] T. Koga, T. C. Harman, S. B. Cronin, and M. S. Dresselhaus, Phys. Rev. B **60**, 14286 (1999).
[6] T. Koga, S. B. Cronin, T. C. Harman, X. Sun, and M. S. Dresselhaus, in *Semiconductor Process and Device Performance Modeling: MRS Symposia Proceedings, Boston*, edited by S. T. Dunham and J. S. Nelson (Materials Research Society Press, Warrendale, PA, 1998), Vol. 490, p. 263.
[7] J. O. Sofo and G. D. Mahan, Appl. Phys. Lett. **65**, 2690 (1994).
[8] P. J. Lin-Chung and T. L. Reinecke, Phys. Rev. B **51**, 13244 (1995).
[9] D. A. Broido and T. L. Reinecke, Phys. Rev. B **51**, 13797 (1995).
[10] D. A. Broido and T. L. Reinecke, Appl. Phys. Lett. **67**, 1170 (1995).
[11] D. A. Broido and T. L. Reinecke, Appl. Phys. Lett. **70**, 2834 (1997).
[12] T. Koga, X. Sun, S. B. Cronin, and M. S. Dresselhaus, Appl. Phys. Lett. **73**, 2950 (1998).
[13] T. Koga, X. Sun, S. B. Cronin, and M. S. Dresselhaus, Appl. Phys. Lett. **75**, 2438 (1999).
[14] T. Koga, X. Sun, S. B. Cronin, and M. S. Dresselhaus, in *The 18th International Conference on Thermoelectrics: ICT Symposium Proceedings, Baltimore*, 1999, p. 378.
[15] T. Koga, X. Sun, S. B. Cronin, M. S. Dresselhaus, K. L. Wang, and G. Chen, J. Computer-Aided Mater. Des. **4**, 175 (1997).
[16] L. D. Hicks and M. S. Dresselhaus, Phys. Rev. B **47**, 16631 (1993).
[17] D. A. Broido and T. L. Reinecke, Appl. Phys. Lett. **67**, 100 (1995).
[18] Z. Zhang, J. Y. Ying, and M. S. Dresselhaus, J. Mater. Res. **13**, 1745 (1998).
[19] Z. Zhang, X. Sun, M. S. Dresselhaus, J. Y. Ying, and J. P. Heremans, Appl. Phys. Lett. **73**, 1589 (1998).
[20] X. Sun, Ph.D. thesis, Massachusetts Institute of Technology, June 1999.
[21] M. S. Dresselhaus, Y. M. Lin, G. Dresselhaus, X. Sun, Z. Zhang, S. B. Cronin, T. Koga, and J. Y. Ying, in *The 18th International Conference on Thermoelectrics: ICT Symposium Proceedings, Baltimore*, 1999, p. 92.
[22] J. L. Liu, C. D. Moore, G. D. U'Ren, Y. H. Luo, Y. Lu, G. Jin, S. G. Thomas, M. S. Goorsky, and K. L. Wang, Appl. Phys. Lett. **75**, 1586 (1999).
[23] T. Koga, Ph.D. thesis, Harvard University, April 2000.
[24] A. Yamamoto (private communication).
[25] K. Seeger, *Semiconductor Physics – An Introduction* (Springer, Berlin, 1985), Chap. 4.
[26] T. Borca-Tasciuc, W. L. Liu, J. L. Liu, T. F. Zeng, D. W. Song, C. D. Moore, G. Chen, K. L. Wang, M. S. Goorsky, T. Radetic, R. Gronsky, T. Koga, and M. S. Dresselhaus, Superlattices Microstruct. (in press).
[27] G. Chen, J. Heat Transfer **119**, 220 (1997).
[28] G. Chen, Phys. Rev. B **57**, 14958 (1998).
[29] T. Borca-Tasciuc and G. Chen (private communication).